



# The effect of $\text{Sr}^{2+}$ on the structure and magnetic properties of nanocrystalline cobalt ferrite

A.C. Lima<sup>a</sup>, A.P.S. Peres<sup>b</sup>, J.H. Araújo<sup>a</sup>, M.A. Morales<sup>a</sup>, S.N. Medeiros<sup>a</sup>, J.M. Soares<sup>c</sup>,  
D.M.A. Melo<sup>b</sup>, A.S. Carriço<sup>a</sup>

<sup>a</sup> Departamento de Física Teórica e Experimental, UFRN, Natal, RN 59078-970, Brazil

<sup>b</sup> Departamento de Ciência e Engenharia de Materiais, UFRN, Natal, RN 59078-970, Brazil

<sup>c</sup> Departamento de Física, UERN, Mossoró, RN 59610-210, Brazil

## ARTICLE INFO

### Article history:

Received 1 December 2014

Accepted 17 January 2015

### Keywords:

Combustion method

Nanoparticles

$\text{CoFe}_2\text{O}_4$

Mössbauer spectroscopy

Magnetic properties

## ABSTRACT

We report the effect of  $\text{Sr}^{2+}$  on the structure, morphology and magnetic properties of  $\text{CoFe}_2\text{O}_4$  synthesized by microwave-assisted combustion method. Results from X-ray diffraction and Mössbauer spectroscopy at 298 K suggest the formation of a mixed spinel  $\text{Sr}^{2+}$  substituted  $\text{CoFe}_2\text{O}_4$ . However, secondary phases like  $\text{CoO}$ ,  $\text{SrCO}_3$  and  $\text{SrFeO}_{2.96}$  were also observed. A decrease in the lattice parameter and particle size were observed with the addition of  $\text{Sr}^{2+}$ . The crystallite size of ferrite phase ranged from 53 to 62 nm. Magnetic studies showed a gradual decrease in the saturation magnetization and remanence with the increase of  $\text{Sr}^{2+}$  content, and an increasing value of the coercive field.

© 2015 Published by Elsevier B.V.

## 1. Introduction

$\text{CoFe}_2\text{O}_4$  is magnetic material with high coercivity field ( $H_c$ ), moderate saturation magnetization ( $M_s$ ), excellent chemical stability and mechanical hardness [1–3], which makes it a potential candidate for many technological applications such as magneto-hyperthermia, magnetic drug delivery, information storage among others [4–6]. The unit cell of spinel ferrite consists of cubic closed packed arrangement of oxygen with 64 tetrahedral (A-site) and 32 octahedral (B-site) interstitial sites, being only 8 A-sites and 16 B-sites occupied by the metal cations. This large amount of empty sites allow the migration of cations between interstitial sites during synthesis. Their physical and chemical properties depend strongly on their composition, structure, shape and particle size, which are affected by the processing method and thermal treatment [7]. The magnetic properties of these materials can be modified by replacing ions located at A and/or B sites [8,9]. The substitution with non-magnetic ions is particularly interesting. For example, Kumar and coworkers synthesized a mixed spinel  $\text{La}^{3+}$  substituted  $\text{CoFe}_2\text{O}_4$  nanoparticles by a citrate method [9] and observed that crystallite size, magnetocrystalline anisotropy,  $M_s$  and  $H_c$  decreased with the increase of  $\text{La}^{3+}$  concentration. The authors concluded that  $\text{La}^{3+}$  have preference for B sites and because lanthanum have zero magnetic moment do not participate in the A–B intersite superexchange, therefore, affecting the magnetic properties. Similar results were found in  $\text{Ca}^{2+}$  doped  $\text{CoFe}_2\text{O}_4$  [10], the authors

concluded that the decrease in anisotropy constant is a consequence of decreasing the exchange interaction of  $\text{Co}^{2+}$  by the addition of nonmagnetic  $\text{Ca}^{2+}$ .

$\text{CoFe}_2\text{O}_4$  nanoparticles have been prepared by several methods including sol–gel [11], thermal decomposition [12], coprecipitation [13], emulsion [14], hydrothermal [15] and combustion [16]. Among these methods, auto combustion reaction has attracted considerable attention due to its convenient processing, simple experimental setup, significant saving in time and energy, and homogeneous products [16].

After reviewing the literature, we noted that there is not any work on  $\text{Sr}^{2+}$  substituted  $\text{CoFe}_2\text{O}_4$  and we believe that it is interesting to study its influence on the structure, morphology and magnetic properties of the  $\text{CoFe}_2\text{O}_4$  phase. Thus, we report the synthesis of nanocrystalline  $\text{CoFe}_2\text{O}_4$  doped with  $\text{Sr}^{2+}$  prepared by microwave-assisted combustion method.

## 2. Experimental

**Synthesis of magnetic ferrites:** Nanocrystalline  $\text{Sr}^{2+}:\text{CoFe}_2\text{O}_4$  ferrites were prepared using  $\text{Co}(\text{NO}_3)_2 \cdot 6\text{H}_2\text{O}$  and  $\text{Fe}(\text{NO}_3)_3 \cdot 9\text{H}_2\text{O}$  as oxidizing agents and  $\text{CO}(\text{NH}_2)_2$  as fuel. Stoichiometric amounts of nitrates and urea were determined based on the total oxidizing and reducing valences of the components, according to the concepts of propellant chemistry [17]. The samples with Sr/Co nominal molar ratio equal to 0, 0.11, 0.42 and 1.0 were named CF, CFS10, CFS30 and CFS50, respectively. For the synthesis, a small

E-mail address: [Marco.MoralesTorres@gmail.com](mailto:Marco.MoralesTorres@gmail.com) (A.C. Lima).

<http://dx.doi.org/10.1016/j.matlet.2015.01.066>

0167-577X/© 2015 Published by Elsevier B.V.

amount of distilled water at 70 °C was used to mix the reagents. In microwave oven, the solution is boiled and its decomposition occurred with copious emission of gases ( $N_2$ ,  $NO_2$ ,  $CO_2$ ). When the ignition temperature was reached, it began to burn and release a great deal of heat producing a brown powder. The time interval for complete combustion process was about 15 min.

**Materials characterization:** The samples were characterized by X-ray diffraction (XRD) using a Mini Flex RIGAKU diffractometer and  $Cu K\alpha$  radiation. The XRD patterns were refined by the Rietveld method using the program MAUD. The crystallite size was determined by using the Debye–Scherrer formula [18]. The morphology of the powders was analyzed on a Phillips XL 30 digital scanning microscope. Mössbauer spectra were recorded at room temperature using a spectrometer from Wiessel with a  $^{57}Co$ : Rh source and activity of 25 mCi. Magnetic measurements were performed at 298 K in a homemade vibrating sample magnetometer (VSM).

### 3. Results and discussion

The XRD patterns of  $Sr^{2+}:CoFe_2O_4$  samples are shown in Fig. 1. Characteristics reflections of  $CoFe_2O_4$  spinel structure (98553-ICSD) was observed. We noticed also the presence of cobalt monoxide ( $CoO$ , 9865-ICSD), strontium carbonate ( $SrCO_3$ , 166088-ICSD) and strontium ferrite ( $SrFeO_{2.96}$ , 172016-ICSD) phases which are paramagnetic at 298 K [19,20]. The Sr related secondary phases increased with the dopant concentration. The crystallite sizes of the pure cobalt ferrite (CF) was 62 nm and for Sr doped  $CoFe_2O_4$  samples were: 53 nm (CFS10), 58 nm (CFS30) and 55 nm (CFS50). Their lattice parameters were 8.3816 Å (CF), 8.3812 Å (CFS10), 8.3787 Å (CFS30) and 8.3776 Å (CFS50). The decrease in lattice parameter is due to the transfer of  $Co^{2+}$  from octahedral sites to tetrahedral sites because of the increased concentration of the  $Sr^{2+}$  in octahedral sites. Excess of Sr accumulates at the grain boundaries as secondary phases, these phases may suppress the grain growth [21]. Kumar and coworkers have

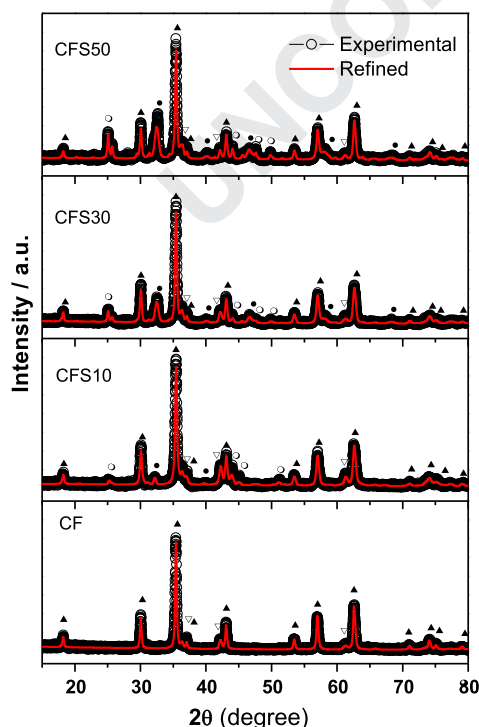


Fig. 1. XRD patterns of  $Sr^{2+}:CoFe_2O_4$  ferrites.  $\blacktriangle$   $CoFe_2O_4$ ,  $\nabla$   $CoO$ ,  $\bullet$   $SrFeO_{2.96}$ ,  $\circ$   $SrCO_3$ .

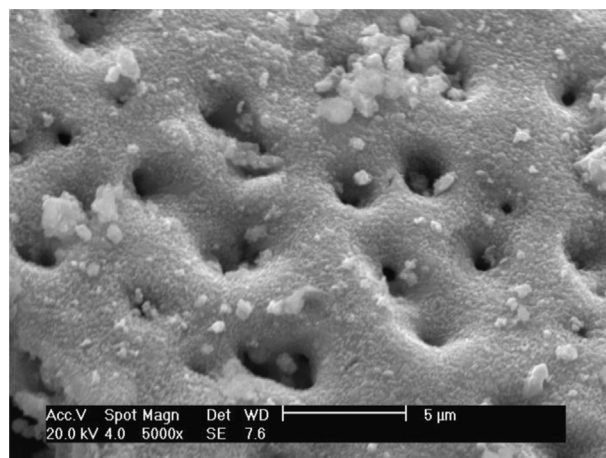


Fig. 2. SEM image of CFS50 sample.

reported that when some  $Fe^{3+}$  are substituted by  $La^{3+}$  in  $CoFe_2O_4$ , the lattice parameters may increase or decrease depending upon two effects, the large size of  $La^{3+}$  tries to increase the lattice parameter and the strain produced by its substitution in the cell, tries to decrease it [10].

Fig. 2 shows the morphology of the CFS50 sample. The picture reveals agglomerates of particles and its surface shows large pores formed by the escaping gases during the combustion reaction. The particles in the agglomerates are smaller than 100 nm corroborating the results from the XRD data.

Mössbauer spectra ( $M_s$ ) are shown in Fig. 3a, each spectrum exhibit four subspectra. Two sextets related to  $Fe^{3+}$  in the octahedral (site 1) and tetrahedral (site 2) sites of the  $CoFe_2O_4$  phase and two paramagnetic components assigned to  $SrFeO_{2.96}$  phase [22]. The doublet (site 4) and singlet (site 3) are related to  $Fe^{3+}$  and  $Fe^{4+}$  occupying octahedral sites in perovskite phase, respectively. Table 1 shows the hyperfine parameters obtained from the fits. The ratio of the relative absorption area (RAA) between site 1 and site 2 reveals values of 3.8 (CFS10), 5.5 (CFS30) and 5.5 (CFS50). These results indicate that doping with Sr favors the Fe octahedral occupancy. In  $CoFe_2O_4$ , most of  $Co^{2+}$  reside on octahedral sites and a small fraction of these ions goes to tetrahedral sites. When  $Sr^{2+}$  are introduced into octahedral sites, the  $Co^{2+}$  migrate to the tetrahedral sites. These  $Co^{2+}$  force equal amount of  $Fe^{3+}$  migrate to octahedral sites, therefore, decreasing the RAA in site 2. The  $SrFeO_{2.96}$  phase showed similar total RAA of  $\sim 29\%$  for samples CFS30 and CFS50, being this value larger than the one for sample CFS10. From the XRD and  $M_s$  analysis we may conclude that excess of Sr allows the formation of the  $SrCO_3$  and  $SrFeO_{2.96}$  phases.

The hysteresis loops for all samples (Fig. 3b) exhibited ferri-magnetic behavior. Their magnetic parameters are shown in Table 1. The hysteresis loops for samples CFS30 and CFS50 have remanence ratio ( $M_r/M_s$ ) of 0.47 which is very close to the value of 0.5 predicted for uniaxial randomly oriented noninteracting single-domain particles [23]. Sample CFS10 has  $M_r/M_s = 0.38$  which can be attributed to an interacting magnetic system [23]. These results seem to indicate that for Sr concentrations above 10%, the paramagnetic secondary phases promote an array of magnetically isolated ferrite nanoparticles. It is observed an increase of  $H_c$  with the Sr concentration, followed by a decrease in  $M_s$  and  $M_r$ .  $M_s$  showed that the concentration of the  $SrFeO_{2.96}$  phase increased, reaching a maximum value for samples CFS30 and CFS50. Thus, we can conclude that the smaller  $M_s$  value for samples CFS30 and CFS50 is related to the mass of the secondary phases, and to spin disorder at the surfaces of nanoparticles. In  $CoFe_2O_4$ , the particle size to form a multidomain system is about

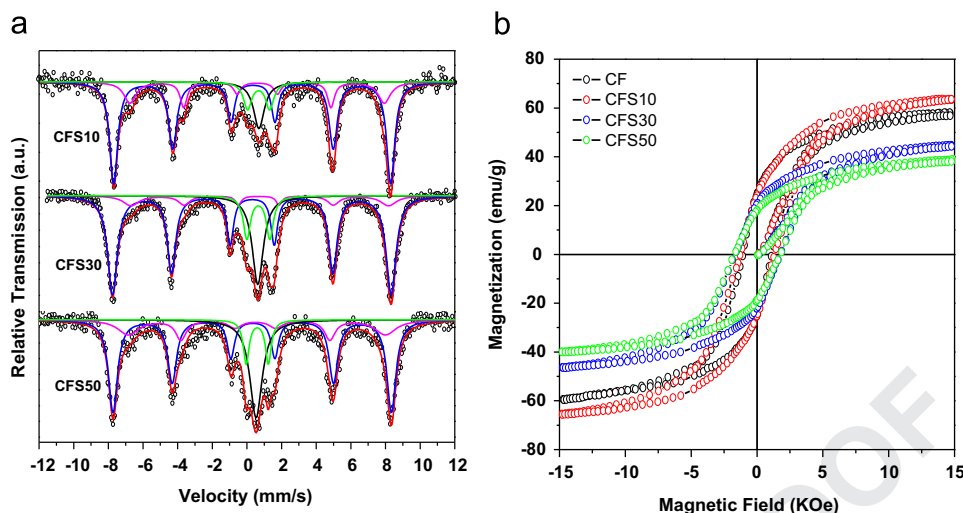


Fig. 3. (a) Mössbauer spectra and (b) hysteresis loops of  $\text{Sr}^{2+}:\text{CoFe}_2\text{O}_4$  ferrites at room temperature.

Table 1

Magnetization and Mössbauer hyperfine parameters of  $\text{Sr}^{2+}:\text{CoFe}_2\text{O}_4$  ferrites.

Samples	$M_s$ (emu/g)	$M_r$ (emu/g)	$H_c$ (kOe)	Sites	Hhf (T)	$\Delta$ (mm/ s)	$\delta$ (mm/ s)	RAA (%)
CFS10	63.4	24.6	1.30	1	49.4	-0.033	0.330	65
				2	45.6	0.117	0.590	17
				3	–	–	0.701	7
				4	–	1.282	0.745	11
CFS30	44.3	20.6	1.71	1	50.6	-0.021	0.326	61
				2	47.8	0.121	0.590	11
				3	–	–	0.679	10
				4	–	1.303	0.732	18
CFS50	38.2	17.9	1.74	1	49.7	-0.027	0.326	60
				2	44.9	0.052	0.532	11
				3	–	–	0.620	12
				4	–	1.355	0.710	17

Hhf is the hyperfine magnetic field,  $\Delta$  is the quadrupole shift;  $\delta$  is the isomer shift.

70 nm [24].  $\text{CoFe}_2\text{O}_4$  crystallites exceeding this size will have very reduced  $H_c$  values. Recent studies have reported coercivity field values up to 1.2 kOe for  $\text{CoFe}_2\text{O}_4$  particles with sizes ranging from 25 to 30 nm, and very small values above 45 nm [25]. In our samples, the  $H_c$  values are about 1.7 kOe. The high  $H_c$  value may be related to pinning of the magnetic moments at the interfaces. In fact, similar results were found in an ensemble of 40 nm size  $\text{CoFe}_2\text{O}_4$  nanoparticles, the results indicated that even at this size scale, single domain magnetic structures are not achieved possibly due to the existence of dominant pinning sites [26].

#### 4. Conclusions

In summary, we have prepared nanocrystalline  $\text{Sr}^{2+}:\text{CoFe}_2\text{O}_4$  ferrites by microwave-assisted combustion method, and the structure, morphology and magnetic properties were examined using different techniques. The XRD analysis showed the formation of a  $\text{Sr}^{2+}$  substituted  $\text{CoFe}_2\text{O}_4$  phase, where the lattice parameter decreased with increasing the strontium concentration. Mossbauer spectra revealed that for the cobalt ferrite phase,  $\text{Sr}^{2+}$  goes mainly to octahedral sites. However, the excess of  $\text{Sr}^{2+}$  favors the production of  $\text{SrCO}_3$  and  $\text{SrFeO}_{2.96}$  paramagnetic phases. The magnetic measurements

showed that when the strontium concentration is increased, the  $M_s$  and  $M_r$  decreases followed by an increase of  $H_c$ . All samples in this study showed secondary phases, these results seem to indicate that strontium has low solubility in the  $\text{CoFe}_2\text{O}_4$  phase.

#### Acknowledgments

The authors wish to thank the Brazilian agency CNPq for the financial support.

#### References

- [1] Li L. J Sol-Gel Sci Technol 2011;58:677–81.
- [2] Liu X-M, Fu S-Y, Xiao H-M, Huang C-J. Physica B 2005;370:14–21.
- [3] Ai L, Jiang J. Curr Appl Phys 2010;10:284–8.
- [4] Kim D-H, Nikles DE, Johnson DT, Brazel CS. J Magn Magn Mater 2008;320:2390–6.
- [5] Pileni M-P. Adv Funct Mater 2001;11:323–36.
- [6] Song Q, Zhang ZJ. J Am Chem Soc 2004;126:6164–8.
- [7] Salunkhe AB, Khot VM, Phadatore MR, Pawar SH. J Alloys Compd 2012;514:91–6.
- [8] Baykal A, Kasapoglu N, Koseoglu Y, Basaran AC, Kavas H, Toprak MS. Cent Eur J Chem 2008;6:125–30.
- [9] Kumar L, Kar M. Ceram Int 2012;38:4771–82.
- [10] Saafan SA, Assar ST, Mansour SF. J Alloys Compd 2012;542:192–8.
- [11] Shi M, Zuo R, Xu Y, Jiang Y, Yu G, Su H, et al. J Alloys Compd 2012;512:165–70.
- [12] Herrera AP, Polo-Corrales L, Chavez E, Cabarcas-Bolivar J, Uwakweh ONC, Rinaldi C. J Magn Magn Mater 2013;328:41–52.
- [13] Kumar P, Sharma SK, Knobel M, Singh M. J Alloys Compd 2010;508:115–8.
- [14] Zhao L, Yang H, Zhao X, Yu L, Cui Y, Feng S. Mater Lett 2006;60:1–6.
- [15] Xiangfeng C, Dongli J, Yu G, Chenmou Z. Sens Actuators B 2006;120:177–81.
- [16] Zhang X, Jiang W, Song D, Sun H, Sun Z, Li F. J Alloys Compd 2009;475:L34–7.
- [17] Costa ACFM, Silva VJ, Xin CC, Vieira DA, Cornejo DR, Kiminami RHGA. J Alloys Compd 2010;495:503–5.
- [18] Cullity BD. Elements of X-ray diffraction. 3rd ed. Prentice Hall; 2001.
- [19] Takeda T, Yamaguchi Y, Watanabe H. J Phys Soc Jpn 1972;33:967–9.
- [20] Zhang Y, Dong F, Liu Y, Fei C, Yin D, Xiong R, et al. Mater Chem Phys 2010;124:1034–8.
- [21] Azhar Khan M, Islam MU, Ishaque M, Rahman IZ. Ceram Int 2011;37:2519–26.
- [22] Adler P, Lebon A, Damjanovic V, Ulrich C, Bernhard C, Boris AV, et al. Phys Rev B 2006;73:094451.
- [23] Stoner EC, Wohlfarth EP. Philos Trans R Soc London, Ser A 1948;A240:599.
- [24] Berkowitz AE, Schuele WJ. J Appl Phys 1959;30:135s–36ss.
- [25] Maaz K, Mumtaz A, Hasanain SK, Ceylan A. J Magn Magn Mater 2007;308:289–95.
- [26] Sheet G, Cunliffe AR, Offerman EJ, Folkman CM, Eom C, Chandrasekhar V. J Appl Phys 2010;107 (104309-104309.6).